Fluorescence yield in N_2 from quantum efficiency to atmospheric conditions

D. Lebrun

ISN-GRENOBLE-Report 02-37

Fluorescence Yield in N_2
From Quantum efficiency to Atmospheric conditions

Didier Lebrun (ISN-Grenoble)

The detection of cosmic Extensive Air Shower via light emission in atmosphere needs a good knowledge of the primary luminescence yield of air molecules under the impact of charged particles and the transmission of the produced light through the atmosphere as well.

In the EUSO Simulation Working Group the handling of the Atmospheric Profile properties was partly devoted to the Grenoble group. It concerns mainly the radiative transfer treatment from the shower site to the ISS, but also it is concerned by the identification of atmospheric parameters whose influence on the EAS profile could be significative.

Apart from usual thermodynamical variables (pressure and temperature), several parameters, such as water vapor and/or aerosols and clouds, can have a severe influence not only on the radiative transfer of light but also on the light production itself. Two main effects are clearly identified: the Cerenkov light yield dependence upon the index of air, and the FluorescenceYield dependence on meteorological conditions.

These two effects argue to consider the atmospheric profile, determined either with standard models or with external data, as a general frame in which the complete shower development simulation should be included.

Here we shall concentrate on fluorescence yield and its dependence upon the various atmospheric conditions where the EAS take place.

Table of content

1. Introduction

A lot of work was already devoted to this subject mainly in the early sixties to study atmospheric phenomena such as auroras, particle physics detectors and already to detect cosmic rays. Later Nitrogen fluorescence was also studied for laser physics and more recently the subject was re-investigated in the perspective of EAS detection. Then various data exist and the status of knowledge in 1967 was compiled in the A.N.Bunner Ph.D. thesis [1] which is still the main reference used nowadays in cosmic shower detection. One has to draw here the attention to the fact that this work is a compilation of experiments (including his own measurements) and an extrapolation via calculations to EAS fluorescence yield estimate under atmospheric model conditions. In 1996 measurement of fluorescence yield in air induced by electrons was performed by F.Kakimoto et al.[2]. It seemed to reveal some discrepancy between the yield they obtained and the yield measured by Bunner [1], while in accordance with the most complete set of data by Davidson & O'Neil [3]. At the contrary they seem in accordance with the expectation of Bunner, say the well known "4 photons per electron per meter"; this contradiction is due to the fact that Bunner himself in his calculations excluded its own measurements and instead chose the Davidson one as a basis.

This contradiction, with other apparent discrepancies from experiments addressing to various aspects of the fluorescence, lead to some confusion ending to the conclusion that fluorescence yield has to be re-measured. That's certainly true but before doing that, it seems necessary trying to clarify the situation in order to know what kind of experiment has to be done.

Many of the listed data were performed under various excitation mechanisms, various wavelength bandwidths due to various filters and photomultipliers, and under various conditions of pressure and temperature, either in pure nitrogen or air, in presence of pollutants or not. The aim of the Bunner thesis was to disentangle among all these parameters in view of EAS detection in atmospheric conditions and for this reason , it is still the main reference on the subject. Nevertheless, in view of the EUSO project, first in view of the Simulation Program and then the Experimental accompanying program, we think that the process of fluorescence in atmosphere has to be revisited, at least at an internal comprehensive and didactical level.

2. General features of Nitrogen fluorescence

From available published data, main features of the air fluorescence can be drawn. Most part of the light produced in air under particle impact is emitted in wavelengths between 300 and 450 nanometers. It consists in approximately 30 individual main lines which were identified with variable intensities upon conditions. Also depending on experimental conditions some lines may overlap.

All these transition lines correspond to Nitrogen excitation and de-excitation transition bands. Only two excited states and decay bands are involved: the First Negative (1N) band corresponding to the $B^2\Sigma_u^+$-$X^2\Sigma_g^+$ electronic transition in molecular ion N_2^+, and the Second Positive (2P) band corresponding to the $C^3\Sigma_u$-$B^3\Pi_g$ electronic transition in neutral N_2 molecule.

The two states are excited through different processes with cross-sections varying differently on the impact energy and the nature of the incident particle. The $B^2\Sigma_u^+$ in N_2^+ is excited through direct process following ionization, while $B^2\Sigma_u^+$ in N_2 proceeds via a two-step process. It has been shown that this process is governed by inelastic scattering or charge exchange reaction of secondary electrons on N_2 . This implies that transport coefficients of electrons in gases has to be considered via Maxwell- Boltzman theory; the effect of electron

attachment is important particularly under the presence of pollutants leading to inhibit the two-step process. Oxygen and water "quenching" will act at this level.
The de-excitation proceeds via radiative transition from state ν in the upper level to the state ν' in the lower one. The transitions to $\nu'=0$ are known as the head of band; for example the 1N(0,0) head transition occurs at λ=391.4 nm, and 2P(0,0) occurs at λ=337.1 nm. The relative intensities of $\nu'\#0$ lines inside a given band are related to the head of band via the Franck-Condon factors.
In competition with radiative decay, the excitation energy can be released through atomic collisions. The rate of this non-radiative decay will depends on the collision rate governed by pressure and temperature of the gas and also by the nature of the gas. The ratio of both rates gives the effective fluorescence yield. The radiative transition rate can be extracted from data obtained at very low pressure (few microns) where the non-radiative decay is minimized. The effective yield is obtained by varying pressure at constant temperature; here only the head of bands have to be measured in principle but overlapping lines have to be carefully checked.
In order to get the light yield in EAS, one has to make a convolution of the above fluorescence efficiency parameters with the molecular excitation rate generated in the shower. The number of molecular ions or molecules in excited states produced per unit length will depends, apart from the medium pressure and temperature conditions, on the nature of the incident particles through their energy loss by ionization and also to their energy distribution within the shower. It will depend on the mean energy to produce an electron-ion pair in the medium and for the two-step process, it will also depend on the energy distribution of the ionization secondary electrons. It is admitted that fluorescence in a shower is produced mainly by electrons and positrons which are by far the most abundant. The electron ionization characteristics are well known and tabulated. F.Kakimoto et al.[2] measured the fluorescence yield in air for various incident electron energies from 1.4 MeV to 1 GeV, the dependence on ionization loss is clearly established. The energy distribution of electrons in showers is of crucial importance since a 80 MeV electron in one metre of air at normal pressure, looses as much energy by ionization as a 400 keV electron does; the only difference lies in the fact that the later stops and the former not. At our present knowledge no precise answer has been found, except that mean electron energy should be around 80 MeV which is the critical electron energy. Previous estimations of the yield used this value as an input basis. The slope of the distribution should have a great importance. Estimation of this distribution could be obtained from Monte-Carlo shower simulations. A differentiation of the empirical formulas describing the number of particle as a function of shower age s leads to a distribution of the kind $dn/dE \# E^{-(s+1)}$[4]. The slope even varies with shower age; electrons being more energetic at the onset of the shower than at the end ! The yield will then vary in accordance during the EAS development. The primary ionizing particle energy induces a variation of the secondary ionization electrons energy distribution which are mainly responsible for the 2P transition in N_2. As a consequence a dependence of the ratio 1N/2P fluorescence yield should be expected as a function of shower age in addition to the local pressure and temperature effect !

3 – Fluorescence characteristics

3.2 Typical Optical spectrum

The fluorescence spectrum consists in approximately 30 lines belonging to the 2 transition bands 1N and 2P.

The different lines are identified to the transitions 1N(ν,ν') and 2P(ν,ν'), the wavelengths of the transitions are listed in Angstrom unit in the following tables.

1N	0	1	2	3	4
0	3914	4278	4709	5228	
1	3582	3884	4236	4652	5149

2P	0	1	2	3	4	5	6	7	8
0	3371	3577	3805	4059	4344	4667			
1	3159	3339	3537	3756	3998	4270	4574		
2	2977	3136	3309	3500	3711	3943	4201	4490	
3	2820	2962	3117	3285	3469	3672	3894	4141	4416

From the intensity picture ones sees that the main contributing transitions lines are the 2P(0,0) at 337.1 nm, 2P(0,1) at 357.7 nm, the 2P(1,0) at 315.9 nm and the 1N(0,0) at 391.4 nm and the 1N(0,1) at 427.8 nm

Here they are shown superimposed, each one being normalized independently. In real experiments the relative yield of both bands can vary according to the conditions.

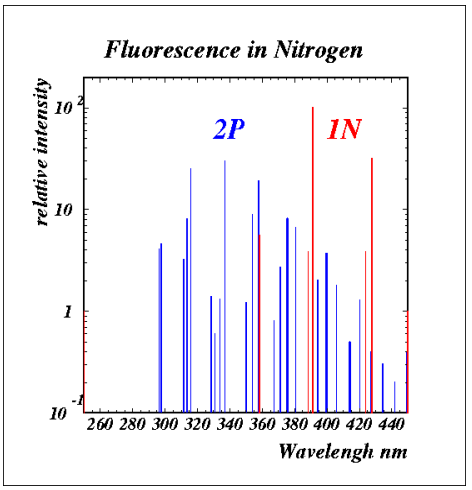

3.3 Photon yield and absolute efficiency

The absolute efficiency **E** is the product of the excitation function **S** of the fluorescence state times the de-excitation rates expressed by the quantum efficiency **Q** [5].

$$E = S * Q$$

It expresses the efficiency to convert the energy of n_i incident particles, each depositing an energy e_i in the system, to excitation energy converted in n_ϕ photons of energy e_ϕ

$$E = n_\phi.e_\phi/n_i.e_i$$

Then the photon yield for one incident electron is obtained from the measured efficiency via

$$n_\phi = E.\ e_i/e_\phi$$

3.4 Measurements and bandwidth effects

Various measurements have been realized, but one can easily understand that the results depend strongly on the bandwidth used in the experiment. In particular if 1N and 2P are mixed within a large band filter, since we know that the 2 bands behave differently under external conditions .The extrapolation of the different results to various atmospheric conditions should be taken with caution.

Usually the measurements were done using a broad band filter **300-400 nm** eliminating the contribution of the 1N(0,1) transition and other transitions above 400 nm; however one has to take care of the filter thickness and transmission coefficient to avoid or take into account edge effects.

For various reasons not linked to the efficiency but to the light transmission in atmosphere it is better to use a **330-400 nm** filter. The absorption of UV light by the ozone layers (either high altitude or tropospheric) starts below 330 nm. In this case the 2P(1,0) transition at 315.9 nm should be strongly affected and locally dependent. Individual lines were studied either with narrow band filters or with spectrometers. Usually the main lines at **337.1**, **357.7** and **391.4** nm were studied , two of them are head of band. It is of main importance to consider the bandwidth of the filters. The overlapping of lines can affect the conclusions. This concerns the 2P(0,1) at 357.7 nm line which overlaps the 1N(1,0) lines at 358.2 nm which differs only by 0.5 nm and whose relative amplitudes vary under excitation conditions. The 1N(0,0) at 391.4 nm measurement can also be affected by overlapping with 2P lines if the width of the filter is large.

For these various reasons we consider here and in the following chapters that, within the band 330-400 nm, the best measurement of Nitrogen and Air fluorescence is the Davidson & O'Neil one [3]. They measured fluorescence at 600mmHg under 50 keV electron impact for individual lines with a spectrometer with $\Delta\lambda$=1.8 nm**.** The overlap of lines was taken into account and measured separately.

Their fluorescence efficiency in air is in agreement within error bars with Kakimoto et al. [2], who measured fluorescence for the 3 main lines with $\Delta\lambda$~12 nm filters under 1.4 MeV electron impact.

The efficiency measurement of Davidson & O'Neil for Nitrogen and Air is shown in the following figure.

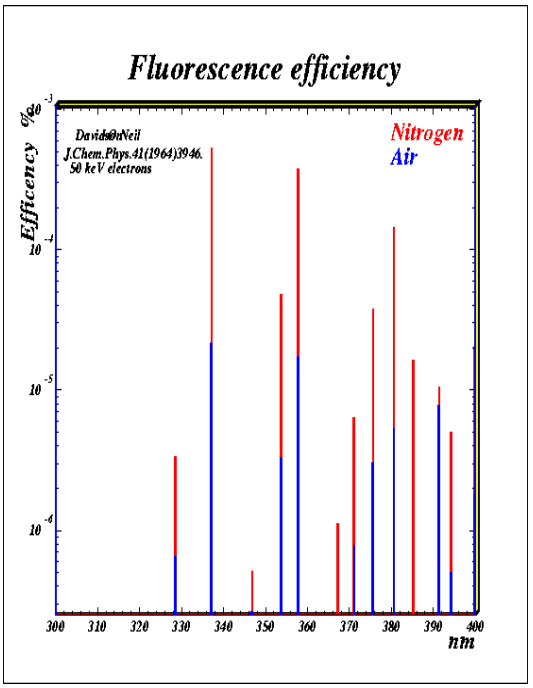

4 Excitation functions

4.1 Excitation of 1N band in N_2^+

4.1.1 Cross-section under electron impact

Emission cross-section for the N_2^+ first negative band has been studied several times under electron impact. We present here the results of ref [6] for 1N(0,v'), other references can be found therein. The onset of cross-section is around 20 eV and the maximum of cross-section occurs around 100 eV . The total excitation at maximum is $\sigma_{1N}=2.38\ 10^{-17}cm^2$

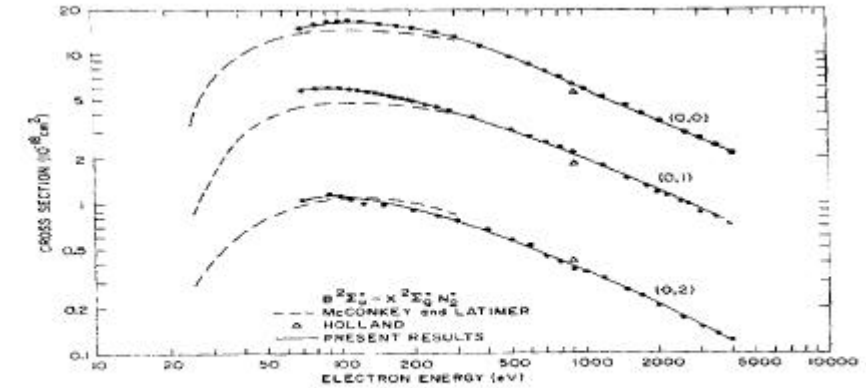

FIG. 2. Emission cross sections of the (0, 0), (0, 1) and (0, 2) first negative bands of N_2^+ by electron impact.

Data of ref [6] are the more accurate found in the litterature, at least for relative cross-section within 1N band under electron impact. This set of data will be used by us in further calculation

4.1.1 Cross-section under proton impact

The optical emission under proton impact from few keV to MeV were also studied. A spectrum is shown for 55 keV protons on N_2 from reference [7]. This spectrum is shown here to illustrate the variation of optical spectrum upon excitation conditions. In the case of proton impact, it is clearly seen that the 1N band is dominant. The 2P band is slightly excited at this impact energy . One can also notice the 3582 line in 1N overlapping with 3577 line in 2P.

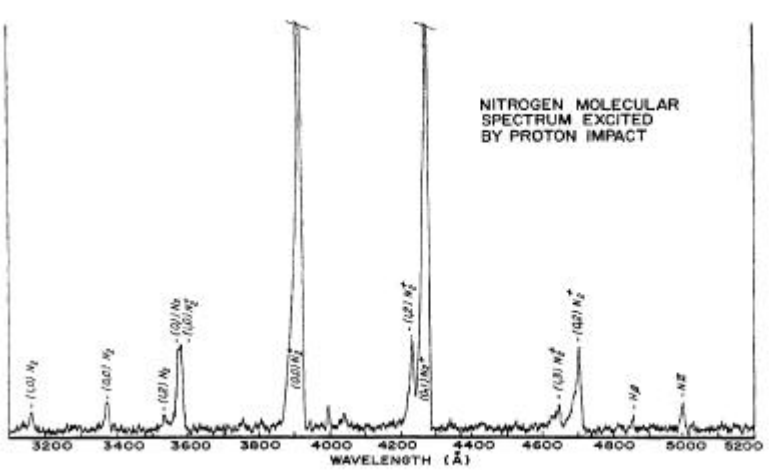

FIG. 6. Spectrum produced by a 7-μA beam of 55-keV protons incident upon nitrogen gas at a pressure of 5.7 μ. Monochromator slits equivalent to 7 Å.

4-2 Excitation of 2P Band in N_2

4-2-1 Cross-section of 2P(0,0) band

Electron excitation was recently revisited in 1996 [8]. Measurements of cross-sections were performed at 0.5mTorr for electron impact energes up to 600 eV. The cross section at maximum is $\sigma_{2P(0,0)}$=1.09 10^{-17} cm^2 for an electron energy of 15 eV and falls rapidly like $(E/15)^{-2}$ as shown in the figure extracted from [8]

The pressure dependence shows a net deviation from linearity above 2 mTorr for incident energy above 100 eV , confirming the fact that the 2P band is populated via **2-step process** involving mainly secondary electrons undergoing charge exchange reaction with N_2 molecule, since the C $^3\Pi_u$ state cannot be excited directly due to electronic spin conservation.

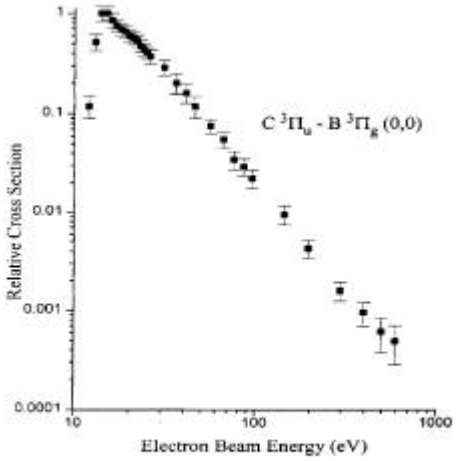

FIG. 4. Relative excitation cross section for the $C\ ^3\Pi_u \rightarrow B\ ^3\Pi_g$ (0,0) band for energies from threshold to 600 eV. The error bars represent the total uncertainty including both the statistical and systematic types.

4.2.2 Relative cross-section within 2P band

Relative cross-sections for the different lines were measured in 1996 by Fons et al. [8]. Results are presented on the following table. Other data are quoted therein and compared to theoretical expectations within the Franck-Condon approximation. It gives a coherent compilation of the data up to now. This set of data will be used by us as input for further estimations of the photon yield

2P	0	1	2	3	4	5	6	7	8
0	1.	.63	.25	.081	.021	.004			
1	.64	.027	.29	.277	.103	.03	.014	.003	
2	.085	.213	.016	.029	.08	.053	.019	.012	.003
3	.003	.046	.038	.018		.015	.0156	.012	.005

Optical emission cross-sections for the 2P band (unit 1.09 10^{-17} cm^2) at incident electron energy corresponding to the peak of excitation function from ref [8].

The relative insensity spectrum of the 2P band corresponding to the table above is shown in the following figure.

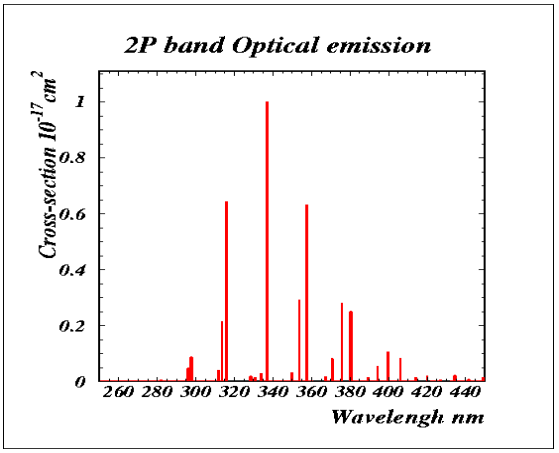

4.2.2 Secondary electron distribution

Since the 2P band is excited preferentially by secondary electrons the total yield will depend on the total number of secondary electrons, which is given by the energy loss by ionization of the incident particle versus the mean energy to create an electron-ion pair, but it should depend also on the energy distribution of these secondary electrons.

The energy distribution of secondary electrons with energy E>>I is given by [10]:

$$dN/dE \simeq (1/\beta^2).F(E)/E^2$$

for $I<<E<E_{Max}$ where I is he Ionization Potential and E_{Max} is the maximum energy of knock-on electrons given by $E_{Max}= 2m\beta^2\gamma^2/(1+2\gamma m/M+(m/M)^2)$

The function $F(E)$ is spin dependent but is approximately 1 for $E<<E_{Max}$.For incident electrons, the indistinguishability of projectile and target means that the range of E extends only to half the energy of the incident particle.

For E close to I, the $1/E^2$ dependence above becomes approximately $E^{-\eta}$ with $3<\eta<5$.

The resulting excitation yield Y of the 2P band is the result of the convolution of cross-section with the distribution of secondary electrons. Above 15 eV $\sigma \sim (E/15)^{-2}$ and for low energy electrons $dN \sim E^{-4}$, the resulting yield $\mathbf{Y(E)\sim E^{-6}}$. This means that Y is strongly determined by the lowest value of σ at 15eV and below; it doesn't vary very much with primary electron incident energy except that the integrated value varies with the upper cut E_{Max}; this last effect can be significant if one considers primary ions with mass M instead of electrons since the E_{Max} expression is then rather different.

4.3 Relative intensity of 1N and 2P Bands at low pressure

If we compare the cross-sections of 1N(0,0) and 2P(0,0) at the maximum of the 1N cross-section around 100eV, with get the ratio (1N)/ (2P)~ 100 while it is ~1 for 20eV.

It is clear that there is a very strong dependence upon impact energy.

Since 2P excitation is mainly due to secondary electrons, the 2P excitation should increase with pressure according also to the energy distribution of these secondary electrons.

5. De-excitation rates

De-excitation of excited states with luminescence is the result of a competition between radiative and non-radiative decays. The luminescence quantum efficiency is the ratio of radiative to all processes. The non radiative part is usually called quenching and involves different ways by which the excited state releases its energy to the lower state of the transition. It can be through non-radiative decay (by emission of particle for example..) or through a decay via an intermediate state; this is known as internal quenching. The excited molecule can release its energy via collisions with other molecule before decaying by radiation, then this rate will depend on density **n** and nature of the collisioning gas. To simplify, one can resume the de-excitation rates to 3 main processes as noted in reference [5]

- Fluorescence rate $\mathbf{k_f}$
- Internal quenching rate $\mathbf{k_i}$
- Collisional quenching rate $\mathbf{k_c.n}$

The corresponding decay times are noted:

$\tau_0=1/(k_f+k_i)$ $\tau_c=1/k_cn_a$ $\tau =1/(k_f+k_i+k_cn)$

$\mathbf{t_c}$ is the collision decay time at atmospheric pressure (STP)

The quantum efficiency with no collision (i.e. obtained at very low pressure) is given by:

$$\mathbf{Q_0=k_f / (k_f+k_i)}$$

While the overall quantum efficiency is :

$$\mathbf{Q= k_f /(k_f+k_i+k_cn) = Q_0 / (1+k_cn/(k_f+k_i))}$$

Assuming a perfect gas law at temperature T , then $\mathbf{n/n_a=P/P_a}$ and

$$Q = Q_0/(1+(P/P_a).(\tau_0/\tau_c))$$

One can defines a **collisional pressure** $\mathbf{P' = Pa \,.\, t_c/t_0}$

Then $\boxed{\mathbf{t = t_0/(1+P/P')}}$ and $\boxed{\mathbf{Q = Q_0/(1+P/P')}}$

5.1 Radiative decay rate

The radiative decay time $\mathbf{t_0}$ has been measured several times ,results are listed in the Bunner work [1]. Disentangling the different experimental conditions, permitting to isolate the non-collisional decay alone, lead to consider the results from reference [9] for the 2 types of transitions as the standard ones :

$\mathbf{t_0\,(1N) = 65.8 \pm 3.5\ ns}$

$\mathbf{t_0\ (2P) = 44.5 \pm 6.\ ns}$

Another compilation (also quoted in ref [1]) gives **67.5 ± 5 ns** and **47.0 ± 8. ns** respectively.

5.2 Internal Quenching

The decay time $\mathbf{t_0}$ (in absence of collisionnal quenching) is given as a characteristic of the transition at a given temperature T. However the population of levels leading to internal quenching of a transition is a function of temperature ($k_i = a.e^{-E/kT}$) and should be rigorously taken into account. It usually leads to an increase of luminescence efficiency as the temperature decreases . For example in Standard Atmosphere the temperature varies from 288 K at ground and decreases to 215 K at altitude of 10-15 km; the internal quenching k_i decreases by a factor of 2. The fluorescence yield should then increase by a large factor in high altitude atmosphere and, above all, should vary along with the shower going down from the top atmosphere to the ground. The quantitative variation of the fluorescence efficiency with temperature due to internal quenching is a function of (k_f/k_i) and , at our knowledge, was not explicitly measured or at least were mixed with collisionnal quenching measurements depending also on temperature and pressure

5.3 Non Radiative Collisional quenching

Collisional quenching occurs when excited molecules loose their excitation energy colliding with molecules in the gas. The rate of these events is given by

$$\mathbf{k_c n = n.s\,.v}\ sec^{-1}$$

Where n is molecule density, σ is the collision cross-section and **v** the molecule mean velocity. The collision cross-sections can be roughly approximed with geometrical cross-section $\mathbf{s = pR^2}$ with R given by the interaction radius (like van der Waals radius). One sees immediately that the cross-sections will then be different if one considers either N_2^+ ions or N_2 molecules impinging on pure Nitrogen molecules. If Oxygen is added like in air, then σ is modified. The collisional rate of 1N or 2P will then be different, a further difference comes from considering pure nitrogen or air.

The velocity distribution of molecules of mass M in a gas at temperature T is given by the Maxwell formula: $\mathbf{f(v) = (M/2pkT)^{3/2} \,.\, exp(-Mv^2/2kT)}$

and the mean velocity $\mathbf{v = (8kT/pM)^{1/2}}$

A typical order of magnitude for collisional rate of Nitrogen with a Radius of 150 Angstroms at atmospheric pressure and 300K gives a collision rate $k_c n \sim 900\ \mu sec^{-1}$ t. This will lead to a collisional pressure P' ~ 1.3 cm Hg for 1N transition and 2cm for 2P. The efficiency Q is reduced by a factor 600 when compared to Q_0 !**]**

The collisional pressure P' is a function of temperature and $\mathbf{P' \# T^{1/2}}$

<u>This collisional quenching is then rather important in gases and depends on the nature of excitation, on the nature and molecular mass of the gas and depends also on temperature.</u>

5.4 Efficiency measurements as a function of pressure

Several measurements of fluorescence yield as a function of pressure where done either in Nitrogen or Air. Results are quoted in reference [1] and [5], they are noted in the following table.

Transition	P' Nitrogen (mmHg)	P' Air mmHg
1N ν=0	1.49	1.08
2P ν=0	90	15.
ν=1	24.5	6.5
ν=2	10.9	4.6
ν=3	5.4	2.5

Once again, results could have been obtained under various conditions of filters and in some cases the temperature is not quoted.

Collisions affect the excited nitrogen state whose excitation energy is released by transfer to other molecules , it should not affect the internal decay scheme of each state. In other words, only the measurement of head of bands would be necessary.

Recent measurements where performed using broad band filters, then mixing 1N and 2P. Measurement in Air and their interpretation should be taken with care and carefully examined depending on the use of natural air or laboratory mixed gases, since other components can affect the results. Interpretation of the variations of yield in air with broad band filters, only in terms of collisionnal pressure effects can lead to misunderstanding since other quenching effects can occur such as Oxygen and/or Water vapor (see next paragraph), which are also transition dependent.

Kakimoto et al.[3] studied pressures and temperature where quoted.

The Palermo group measured Nitrogen and Air fluorescence yield via 22 keV X-rays, varying pressure from 1mbar to atmospheric pressure at 295K constant temperature [ ] .Measurement where performed via a wide band BG1 filter between 300 and 400 nm. Data where fitted with a global collisionnal pressure dependence term.

As an example we used the collisonnal pressure for Nitrogen given in table above and applied it to individual transitions 1N and 2P , in the experimental conditions quoted by the authors: 22 keV electron impact and 295K. and PMT efficiency and filter transmission . The result is shown in the following picture: <u>no adjustable parameter was necessary.</u> Dots are for calculations for 1N(red), 2P(blue) and total (black) light yield; pink triangles are data crudely extracted from the figure in the article

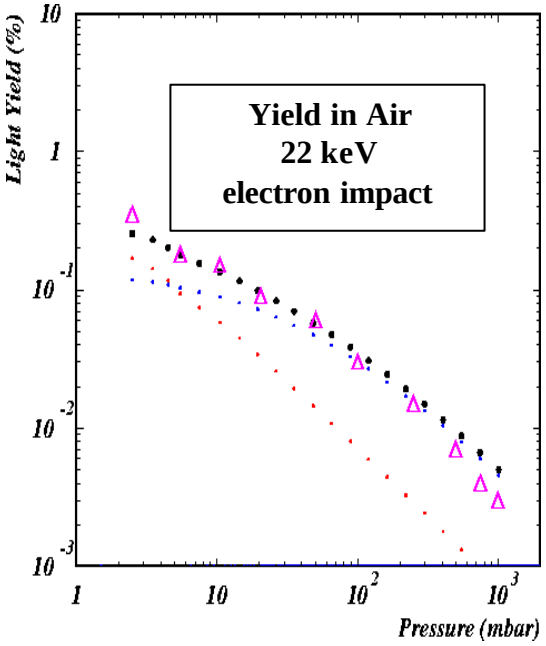

Results in Air could be obtained in two ways : the first one using the collisionnal parameters for Air given in the table above, the second one using the parameter for pure Nitrogen but applying an Oxygen quenching as defined below. Then in the second way no adjustable parameter was necessary.

As a consequence of collisionnal quenching the yield and the spectrum of fluorescence in atmosphere vary with altitude. The atmosphere profile shows a usual exponential decrease with altitude, but also a decrease of temperature from 300 K at ground to 200 K at 10-15 km depending on latitude, longitude and season.
Due to the large difference in collisionnal quenching for the 2P and 1N transition ,the fluorescence nature changes with altitude: it is dominated by 2P for high pressures and by 1N at low pressure. The photon yield spectrum as a function of altitude is presented in the following picture,where individual line contributions are plotted every 4 km..The total transition strength(black) is shown in lower right picture together with the integrated strength for both 2P (red) and 1N(blue) transitions. Region where both transitions contribute for the same amount is located around 30 km, depending on atmospheric profiles. Since wavelengths of both transitions are different, one can observe a shift in the mean wavelength of fluorescence yield from 391 nm and at very high altitude to the lower wavelengths of 2P transitions at low altitude.

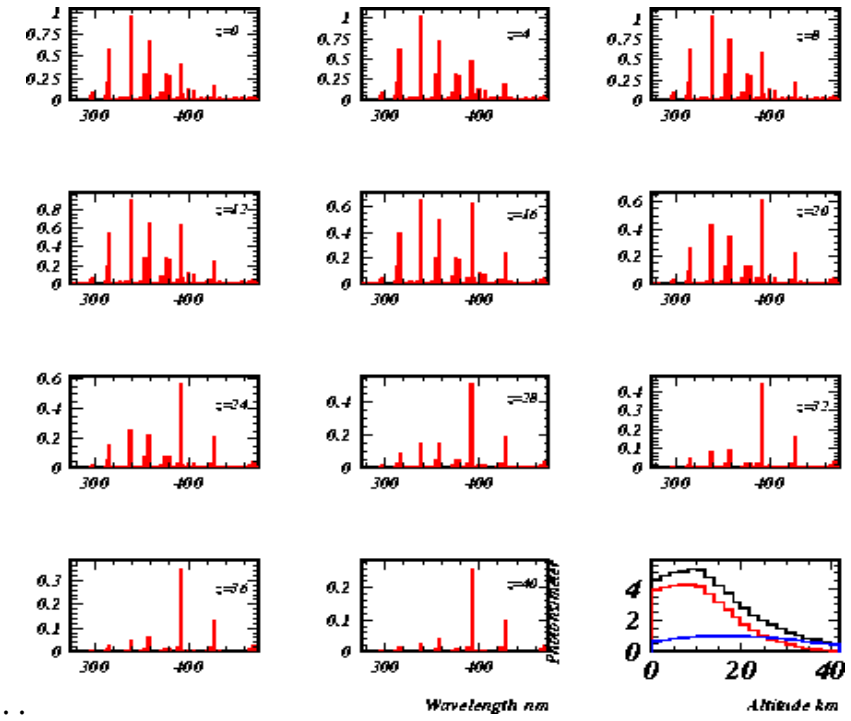

6 Electron attachment in Oxygen and Water Vapor

Electron attachment affects the excitation rate of states which are mainly populated via interaction of low energy electrons .This is the case for the 2P transition and not for the 1N.

6.1. No effect for the 1N transition band

Since the 1N transition is excited through the direct process of ionization, and since oxygen do not present any absorption for the wavelength of 1N transition one can predict that the 1N fluorescence is not affected by the presence of oxygen in air. The only variation of the measured efficiency comes from the lower concentration of Nitrogen in air (79%) and from a difference in mean energy to create a pair in N_2 and O_2.(W_i=35.8 eV and W_i=32.2 eV respectively). The reduction of 1N yield is then expected to be roughly

Yield(1N,Air)/Yield(1N,N2) = 0.79 * (35.8/35.0) = 0.81

6.2. Strong effect for 2P transition band

It is known from the study of gas detectors in particle physics, that transport of electrons under electric field (or not) are strongly affected by the presence of electronegative pollutants at a level of few part per million. Among pollutants Oxygen and Water vapor are the most efficient "quenchers". One example of attachment rate measurement under Oxygen concentration is shown in next figure. Standard values are tabulated as input for Maxwell- Boltzmann codes used in drift chambers [Magboltz]

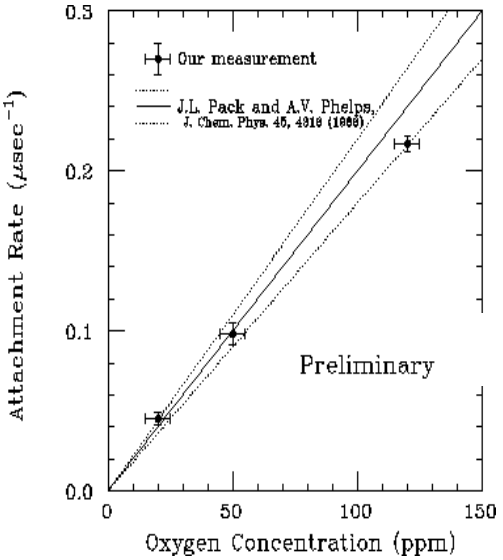

The attachment rate is $\mathbf{t_a \sim (2000 \pm 10\%)*C_{O2}\ msec^{-1}}$.

In Air the concentration of N_2 is 79% and O_2 21 %. When normalized to 1 for N_2, the relative concentration of O_2 is 26.6%. The attachment rate is then $\mathbf{k_a n}$ =530 μsec^{-1}. The quantum efficiency is then reduced from pure nitrogen to air in the same manner as :

$$\mathbf{Q = Q_0 / (1+k_a n/(k_f+k_i))}$$

Only the 2P state is concerned (with τ_0=44.5 ns) and

$$\mathbf{Q_0/Q = (1+530*44.5\ 10^{-3}) = 24.5}$$

This quenching factor of 24.5 for the 2P band due to the presence of oxygen is the one observed by Davidson and O'Neil [2]. They measured also a reduction factor of 0.7 for the 1N(0,0) transition while 0.8 was given above.

This attachment rate in Oxygen is due to the strongly peaked cross-section of O^- formation under electron impact around 6.8 eV (see figure). This is the dominant process of attachment as mentioned in reference [].

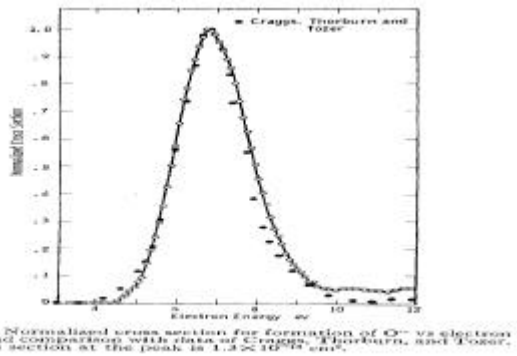

FIG. 5. Normalized cross section for formation of O^- vs electron energy and comparison with data of Craggs, Thorburn, and Tozer. The cross section at the peak is 1.2×10^{-18} cm².

6.3 Attachment due to Water Vapor

The peak of cross-section for electron attachment in water vapor is located at the same energy than the similar cross section in oxygen. Here the dominant process lead to the formation of H^- in water. However the cross-section is 5.4 times higher than in Oxygen.

Since the energy distribution of electrons is the same as in the case of oxygen, the electron attachment rate scales like the cross sections, and consequently it is 5.4 times greater in water than in oxygen. The effect in atmosphere can be very important. As an example a water vapor pressure of 6 mmHg (which correspond to 50% humidity at 15 degrees) lead to quenching factor of :

$Q_0/Q = 1+ (6/760)*2000*5.4*(44.5\ 10^{-3})$

Quenching factor = 4.8

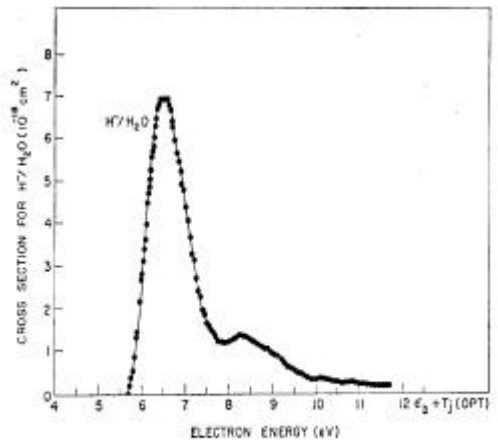

FIG. 2. Electron-capture cross section as a function of energy. Atomic-hydrogen negative ions from water.

7. Argon contribution revisited

From typical molecular concentration in Ambient U.S. Standard Atmosphere [ ] , the main components of air are Nitrogen (.781), Oxygen (.209), Water (.0775 variable) and Argon (.0093). Argon, as all rare gases, is a very efficient scintillator emitting in the far UV at λ~220nm. A priori, it has no direct influence in the bandwidth we consider here. But it is also well known that a nitrogen concentration of 10^{-5} in argon is sufficient for nitrogen bands to appear in the emission spectrum. This was extensively studied and it was shown that there is a transfer of excitation in Argon to excitation in Nitrogen. The transfer mechanism is complex, from UV light emission and re-absorption at higher wavelength to molecular collisions. Whatever the nature of transfer, the effect was used to build Argon scintillation detectors with Nitrogen added acting as a wavelength shifter. Due to excitation energy levels in Argon, transfer only occurs to the $C^3\Pi_u$ state in N_2 and then only the 2P band can be excited, and not the 1N in N_2^+

Scintillation efficiency of argon-nitrogen mixture as a function of N_2 concentration were studied in the range 0 to 100%. Results from Grun and Shopper cited in [ ] are presented below. These results were confirmed later in gas detectors studies. One sees that both pure gases (100%) have almost the same efficiency. Scintillation increases in Argon up to 3% Nitrogen concentration and then decreases with a law

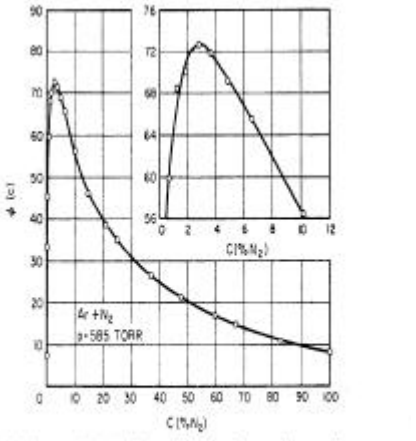

FIG. 14.7. Relative practical scintillation efficiency of argon–nitrogen mixtures as a function of N_2 molar concentration, at $p = 58.5$ cm Hg and 20°C (Grün and Schopper, 1954).

$I=63.5 \exp(-C_{N2}/43.3)$. In Air we are concerned by the right hand side of the curve. Assuming first that Oxygen has no effect in the problem, the relative

concentration of Argon versus Nitrogen in air is (.0093/.781)~1.2%. Scintillation efficiency will then increase from pure 100% N_2 to 98.8 % N_2 by a factor exp(1.2/43.3) ~ 1.028. One can conclude here that Argon in Air can contribute at maximum level of 2.8% of N_2 scintillation efficiency.
A.N. Bunner estimated the effect to 1% then negligible when compared to the overall precision
.
But 2 important remarks have to done :

- The 2P state in N_2 is excited via upper level in Argon via a process like collision but may be not by secondary electron charge exchange; then the very large quenching due to attachment by Oxygen or water in Air doesn't apply here.
- The Grun&Schopper experiment was performed with an S11 type photocathode PMT. They observed the onset and quenching luminescence of argon-nitrogen mixtures for wavelengths above 380 nm (this has to be checked). Since only the 2P transition band can be observed, the fraction of light emitted above 380 nm accounts for only 20 % of the 2P luminescence in the bandwidth 330-400 nm. The effect should have been 5 times greater in the total bandwidth.

One conclusion has to be drawn. A crude estimate of both effect mentioned in the remarks above will lead to an Argon contribution enhanced by a factor more than 100 !
This would lead to an increase of the overall yield in air by at least a factor 2.

This has to be confirmed with more work on existing data. It is obvious that new measurement within the correct bandwidth has certainly to be done.
One can worry also about previous yield efficiency measurements in air: were they done with real air or with industrial gas mixture even with good nitrogen/oxygen proportion but not with the same amount or Argon concentration ? At our knowledge in the Air fluorescence measurement by Davidson and O'Neil [3] the Argon concentration was measured by flame analysis to 670 ppm; this could have lead, if all effects were taken into account, to an overestimation of their 2P efficiency by less than 5% compared to their 15% total error estimate.

8. Photon yield in Extensive Air Shower

8.1 Photon yield under electron impact

For given conditions of Pressure , Temperature and pollutants concentration, the quantum efficiency is fixed and the photon yield varies as the number of ion-electron pairs formed in the collision. For ionization process this number varies as the energy loss by ionization of the incident particle dE/dx. These values are tabulated for electrons in Nitrogen, oxygen and air. Converting to the energy loss per metre one obtains the photon yield per electron per metre as a function of incident particle energy as shown in the figure below.

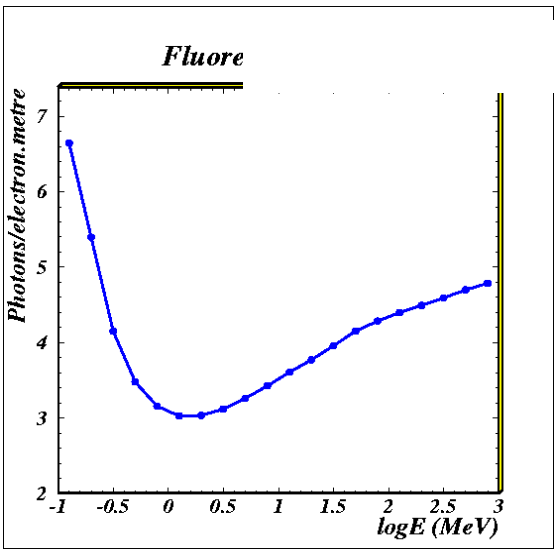

Few remarks have to be done:

- Only the ionization loss has to be considered; radiation loss doesn't generates ions (at least when one compares 1 metre of air with the radiation length)
- For low energy electrons which stop in 1 metre of air, the number of ions created is proportional to E instead of $\delta E/\delta x.\Delta x$; in general one takes $\text{Min}(E, dE/dx.\Delta x)$.
- Calculations have been performed with the conditions of quantum efficiency [3] and collisional pressure indicated in previous chapters. The bandwith considered was 330-400 nm.
- F.Kakimoto et al.[2] performed the measurement at various incident electron energies from 1.4 MeV to 1 GeV. They used a 300-400 nm filter. Correcting for the transition at 315.9 nm which is missing in the 330-400 nm band we used, the results are in perfect agreement.
- The mean value of the obtained distribution lies around 4.2 photons/electron.metre for an incident energy of E~80 MeV. These are called 'Magic Numbers'

8.2 Photon yield in EAS at atmospheric pressure

If we assume that the energy distribution of the electrons at any given stage of the shower development to be $dn/dE \sim \exp(-E/80)$, where 80 MeV is the critical energy of electrons

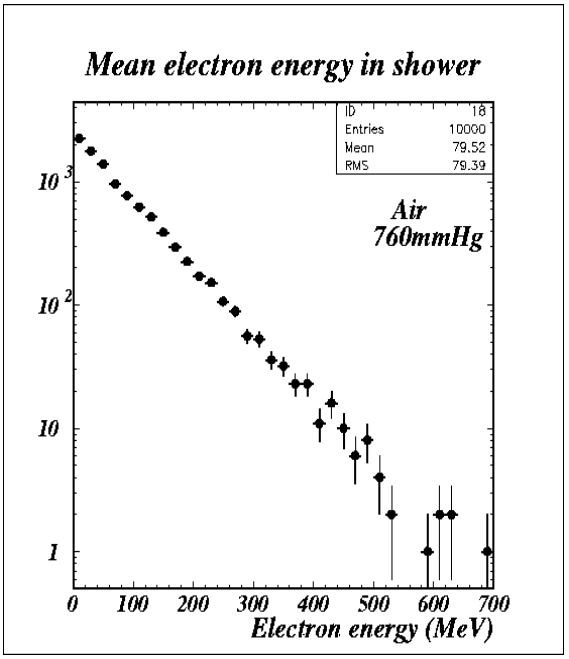

The photon yield in one metre of a shower at atmospheric pressure is given with 10000 electrons trials by:

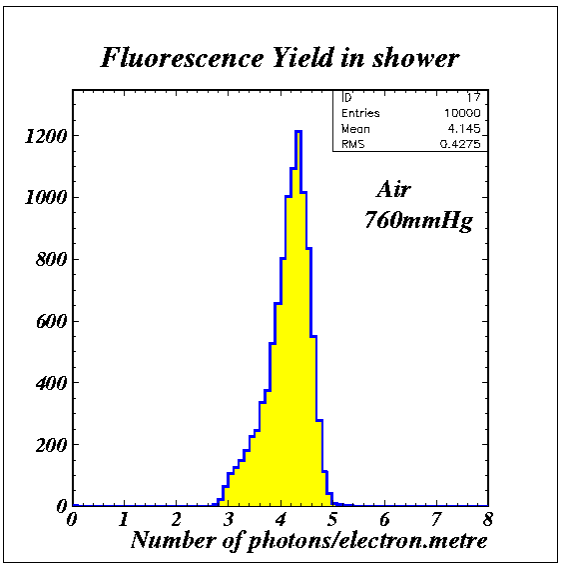

The mean value obtained is

Y = 4.15 ± 0.43 photons/e.m

The width is mainly determined by the slope of electron distribution

8.3 Atmospheric conditions

Assuming 80 MeV as a mean energy of electrons in a shower, we have estimated the photon yield for various dry atmospheres depending on latitude, longitude. Here are presented the results for an equatorial (left) and southern (right) latitudes. The 2 locations are compatible with the ISS trajectory; they will be separated in time by less than 23 minutes. Light yield spectra are shown folded with optical filters supposed to be installed on EUSO telescope (left inset). The upper right insets show the yield vertical profile for both 2P and 1N transition and for the total yield. One observes a clear variation of the yield mainly below an altitude of 15 km ;this is due to the quiet different atmospheric temperature profiles at these 2 latitudes together with slight different geopotential density profiles.

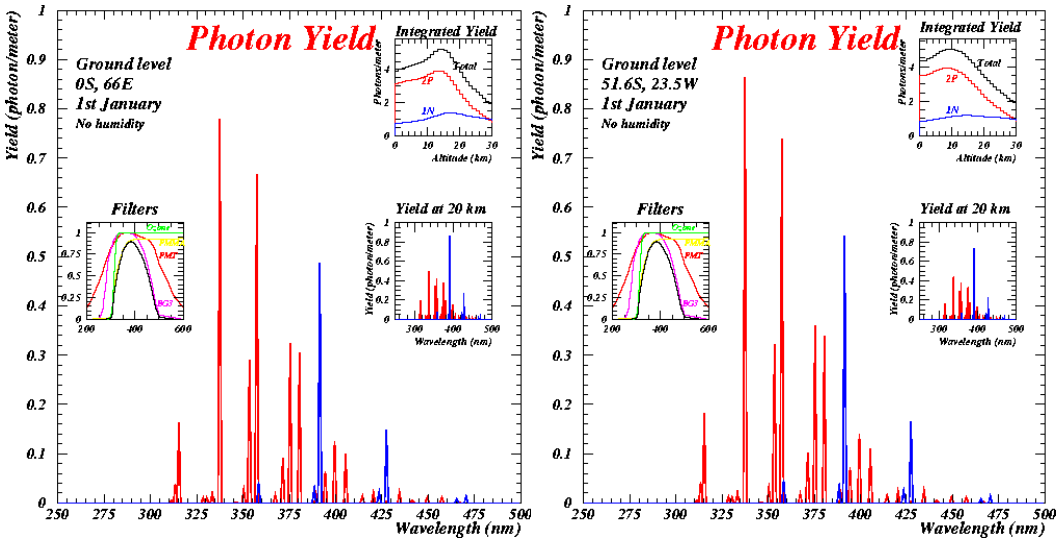

The atmospheric pressure profile doesn't only affect the shower development itself, but the photon yield will vary in an almost independent way along the shower path.

8.4 Water vapor profile in atmosphere

Water vapor profile is usually given in terms of Relative Humidity H Humidity percentage is related to Saturated Waver Vapor Pressure at temperature T by

$H = 100.\ P_w/P_{ws}$

Where P_{ws} is the saturated vapor pressure at given temperature T.
P_{ws} is deduced from the Clausius-Clapeyron formula describing isothermal change of phase. At the triple point (~0.0098 degree C) P_{ws}= 6.11 millibar. The Latent Heat of water over water is L=2.5 10^3 Joule/gram (L=2.82 for water over ice), leads to an expression for the Saturated Vapor Pressure : **$P_{ws}=6.11 \cdot exp[5417(1/T_0 - 1/T)] = 2.504\ 10^9 \cdot exp[-5417/T_K]$ millibars**
On the left figure below are shown profiles of pressure, temperature, ozone and humidity for various US Standard Atmosphere. The water vapour quenching of fluorescence yield was estimated and and the Yield profile is shown in the figure at right below for US-standard profiles with no Humidity (US Standard Dry), applying the quenching with the humidity profile for the same atmosphere and then comparing with Tropical atmosphere. Near ground the variation reaches 30%

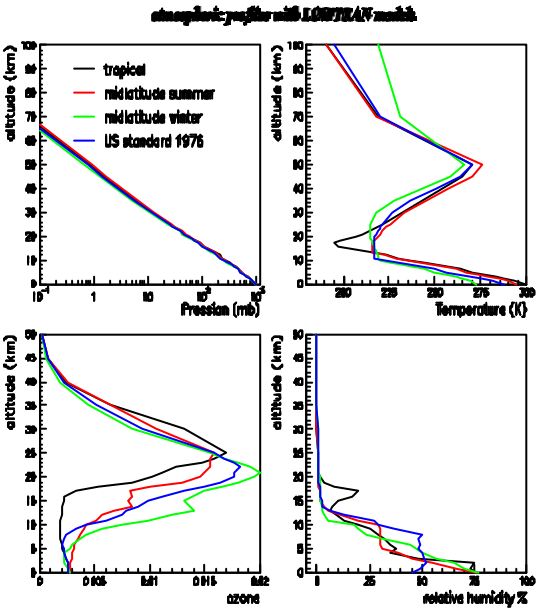

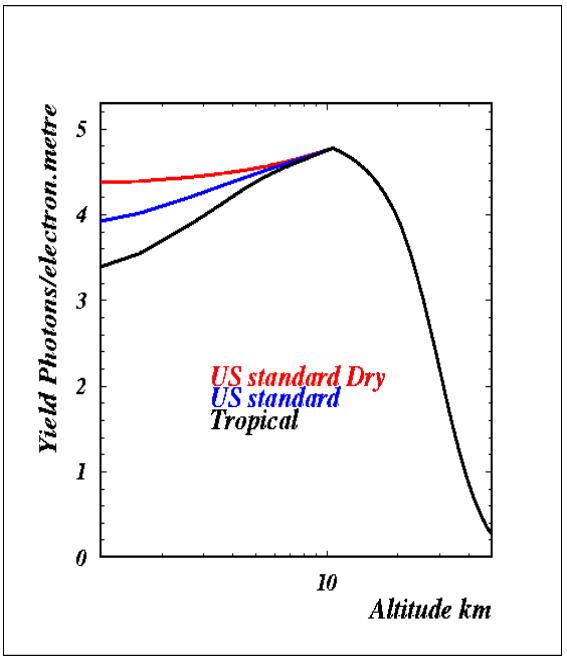

8.5 Dependence of Yield on Shower age ?

The mean photon yield in a shower is a function of the energy distribution of electrons in a shower. The effect is presented for the mean photon yield calculated at atmospheric pressure. Four energy distributions of electrons (above 500 keV)are compared which demonstrate the importance of the knowledge of the real distribution.

Keeping in mind the yield as function of incident energy described in $8.2, one sees that the first distribution is sensitive to high energy electrons with a mean at 80 MeV. The second one (1/E) is 'rather flat' and the 2 bumps reproduce the energy dependence on dE/dx in $8.2 . The other two enhance low energy electrons contribution for E~1MeV (since there is a threshold at 0.5 MeV). Electrons below 500 keV were not considered here, but one can imagine their increasing contribution if they are present in the shower.

If the distribution of electrons is a function of shower age as [4] :

$$dN/dE \# (1/E)^{s+1}$$

then the photon yield will vary along with the shower development.

Electrons are more energetic at the onset of the EAS (s=0) and behave like 1/E, and they become less and less energetic as the shower develops to reach the maximum (s=1) to the very end (s=2). The mean value decreases by ¼ during the shower; with a 'strange' behavior (2 bumps) at the beginning.

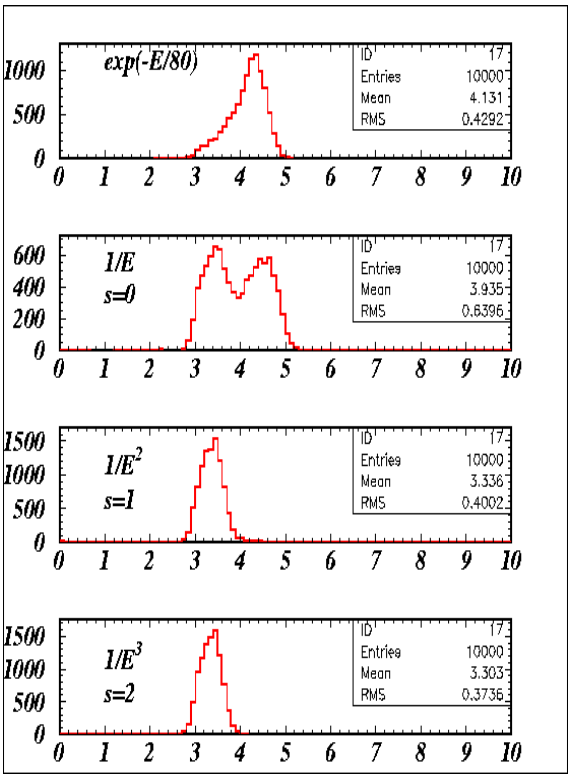

More complete calculations are needed to conclude, with realistic EAS within realistic atmosphere. These are underway

References

1 A.N.Bunner, PhD Thesis, Cornell University, 1967
2 F.Kakimoto et al., NIM A372 (1996) 527.
3 G.Davidson and R. O'Neil, J.Chem.Phys. 41 (1964) 3946.
4 T.K.Gaisser 'Cosmic Rays',
5 J.B.Birks, "The theory and practice of scintillation counting", Pergamon Press,1964
6 B.N.Srivastava and I.M.Mirza Phys. Rev. 176 (1968) 137.
7 D.A.Dahlberg et al. Phys.Rev. 164 (1967) 164.
8 J.T.Fons et al. Phys.Rev.A53 (1996) 2239.
9 G.J. Shultz, Phys.Rev. 128 (1962) 178
10 R.N.Compton and L.G.Christoforou, Phys.Rev. 154 (1967) 110
11 Review of Particle Properties, Phys.Rev. D50 (1994) 1251.